Biomedical Signal Processing and Control 57 (2020) 101674

Contents lists available at ScienceDirect

Biomedical Signal Processing and Control

journal homepage: www.elsevier.com/locate/bspc

Quantitative lameness assessment in the horse based on upper body movement symmetry: The effect of different filtering techniques on the quantification of motion symmetry

F.M. Serra Bragança [a,*], C. Roepstorff [b], M. Rhodin [c], T. Pfau [d], P.R. van Weeren [a], L. Roepstorff [c]

[a] Department of Equine Sciences, Faculty of Veterinary Medicine, Utrecht University, Yalelaan 112-114, NL-3584 CM Utrecht, the Netherlands
[b] Equine Department, Vetsuisse Faculty, University of Zurich, Winterthurerstrasse 260, CH-8057 Zurich, Switzerland
[c] Department of Anatomy, Physiology and Biochemistry, Swedish University of Agricultural Sciences, Uppsala, Sweden
[d] Department of Clinical Science and Services, The Royal Veterinary College, Hawkshead Lane, North Mymms, Hatfield, AL9 7TA, UK

ARTICLE INFO

Article history:
Received 12 December 2018
Received in revised form 22 August 2019
Accepted 16 September 2019

Keywords:
Horse
Signal processing
Lameness
Filter
Asymmetry

ABSTRACT

Quantitative gait analysis in horses is rapidly gaining importance, both clinically and in research. The number of available systems is increasing, but the methods of signal analysis differ between systems and research groups. Our objectives are to describe and evaluate the effects of different methods of signal analysis for processing of data from equine kinematic gait analysis. To this end, we use theoretical signals based on previously published work, followed by the evaluation of the performance of each technique using real data from horses with induced lameness. Two infinite impulse response (IIR), high-pass filters (Butterworth and Chebyshev), a signal decomposition method and a moving average filtering technique were evaluated. First, we describe methods to fine-tune each filter to the optimal settings based on residual analysis. Second the performance of each filter is evaluated based on differences in calculated symmetry parameters from horses with induced lameness. We show that optimisation of filtering techniques is crucial when processing signals used for objective lameness quantification. Improper selection of the cut-off frequency for IIR filters can result in false negative results (average values above or below predefined reference values). The IIR Butterworth filter and the signal decomposition method achieved the best reduction of unwanted signal components. Knowledge of the available filtering techniques is a pre-requisite for adequate signal processing of gait data from quantitative analysis systems in horses.

1. Introduction

Quantitative gait analysis in horses is a long-standing technique in research, but is now rapidly becoming very popular as an objective method to detect and quantify gait abnormalities in a clinical setting [1,2]. It provides the veterinarian profession with objective and unbiased gait information that can be used during the clinical examination of horses presented with problems of the locomotor system, aiding the veterinarian in the localization and diagnosis of orthopaedic problems and offering a unique opportunity for the objective monitoring of the effect of diagnostic or therapeutic interventions. Presently, objective lameness assessment in horses is generally based on the identification and quantification of movement asymmetries of the vertical displacement/acceleration of the head [3–6], withers [3,6–8] and pelvis [9–12] during straight line locomotion at the trot. This is further explained in the background section.

Errors related to kinematic measurements in equine gait analysis can result from a variety of factors including: (a): improper sensor or marker placement [13,14] and Serra Braganca et al. 2017) ; (b): effect of skin displacement [15,16]; (c) improper recording settings (e.g. frame rate) [17] and, in case 3D motion capture is used as the technique, improper number of cameras, marker size and tracking algorithms [18]. These factors are well-known, and measures to minimise them form part of most kinematic measurement protocols. Nevertheless, all raw kinematic data collected in a biological setting using any instrument will, due to confounding factors, ultimately contain a certain number of unwanted components [4] that affect the signal, necessitating a treatment to allow for the accurate calculation of relevant kinematic parameters [18–20].

* Corresponding author.
E-mail address: f.m.serrabraganca@uu.nl (F.M. Serra Bragança).

https://doi.org/10.1016/j.bspc.2019.101674
1746-8094/

One important unwanted component in the vertical displacement signal (VDS) of the head, withers, or pelvis in horses is the displacement offset for the different strides caused by extraneous non-cyclical motion (for instance caused by the animal raising/lowering its head) that is unrelated to the primary locomotion symmetry and which might obscure the original sinusoidal motion signal. Other unwanted components can be an offset in the displacement caused by a slope on the surface the horse is measured when measuring with optical motion capture. The presence of these unwanted components, renders the interpretation and quantification of motion symmetry problematic [4]. Data are therefore routinely processed using a variety of filter techniques.

The effect of different filtering techniques, used for determination of the VDS has been hypothesised as a possible source of differences in between-stride variation (i.e., variation in motion symmetry between consecutive strides) among different publications [21]. However, to the authors' best knowledge, the topic has never been investigated to some depth.

The objectives of this manuscript are to describe and evaluate the performance of different commonly used signal analysis techniques/filter methods using theoretical and real signals of the VDS measured in clinically lame horses. We aimed to establish the optimal configuration for each filter and to assess to what extent the original signal can be distorted and how this might affect the clinically relevant gait parameters that are used for data interpretation. To this end, the manuscript is structured as follows:

1) Description, evaluation and comparison of different methods for filtering VDS data.
2) Proposition of optimal filter settings that should be used when processing VDS data.
3) Comparison of the effect of each filter on real data from horses with induced lameness.

2. Background

2.1. A theoretical representation of the VDS of a trotting horse

During trot, the upper body segments (head, withers, sacrum) describe a sinusoidal curve with twice the frequency of the stride cycle, *i.e.* the head, pelvis and withers move up and down twice during a full stride [3]. This movement can be thought of as a sum of 2 harmonics (H1) and (H2) (Fig. 1). H1 has the same frequency as the stride frequency of the horse (w_s), and H2 has twice the stride frequency:

$$y_t(t) = A_1\cos\left(w_s t + \theta_2\right) + A_2\cos(2w_s t)$$

Where A_1 is the amplitude of the H1 and A_2 is the amplitude of the H2 component of the signal, w_s is the stride frequency and θ_2 is the phase of H1 relative to H2. In a perfectly symmetrical movement H2 is the only component of the signal. A detailed description and deduction of this equation can be found in Appendix A.

When a horse is experiencing prominently unilateral orthopaedic pain, the motion cycle of vertical displacement becomes asymmetrical [3,22] and the first harmonic of the signal (H1) increases in amplitude. This results in a reduced amplitude of the VDS during the stance phase of the lame limb, and an increase on the opposite diagonal [3]. As a consequence of this difference between diagonals, the VDS becomes asymmetrical and several symmetry parameters can be used to quantify this asymmetry [23].

3. Methods

3.1. Initial investigation: filter evaluation and design methods

Several methods to remove the unwanted components present in the VDS have been described in the literature for equine gait analysis including high-pass digital filters like the Butterworth and Chebyshev filters, analysis of the Fourier coefficients [24] and a signal decomposition method [4].

We have generated a theoretical asymmetrical VDS mimicking the motion observed in lame horses, having a frequency of H1 and H2 of 1.5 Hz and 3 Hz respectively, sampled at 200 Hz, with a signal length of 12 s. To this, with added unwanted low-frequency components (noise), in order to mimic data described in the literature [4] (Fig. 1).

3.2. Digital IIR filters

Since the noise signal frequency is lower than the frequency of the first and second harmonic an high-pass filter could be applied. We started by comparing two infinite impulse response (IIR) filters that can be used to remove this low-frequency noise, the Butterworth filter and the Chebyshev type I filter (Supplement, Fig. 1). IIR filters have been extensively used to filter VDS from horses during trot [25–28]. Both filters were applied using a zero-phase filtering technique using the Matlab (MathWorks, Natick, Massachusetts, USA) function 'filtfilt'. To investigate the effect of the filter transients and to mitigate this problem, we have evaluated both IIR filters using a padding technique that fills both edges of the signal, with an artificial signal. This operation was performed by autoregressive modelling using the Matlab function 'fillgaps'. For this model, the padding length was defined as 25 % of the original length of the signal on each edge.

3.3. Design of the analysis of signal decomposition method filter (SDMF)

SDMF is based on the principle described by [4]. This approach uses a curve fitting operation to estimate the three components of the VDS (H1, H2 and the unwanted component). The filter was designed according to the following algorithm.

1 A window for the data analysis is initiated. The window length corresponds to two complete stride cycles, which allows for complete discrimination between the three components of the signal. The window length can be defined by stride events when available or using a fast Fourier transformation (FFT) on the VDS to find the frequency of the two harmonics, H1[w_s] and H2[2 w_s]. Using the sampling frequency (Fs) and the stride frequency (w_s), the window length can, therefore, be defined as:

$$window_{length} = \frac{2\pi.Fs}{w_s}$$

2 A fast Fourier transformation (FFT) is then performed on the VDS within the window to find the specific frequency of the two harmonics (H1[w_s] and H2[2 w_s]).
3 For each window, a curve fitting operation is performed on the measured VDS using a non-linear least squares approach and the equation previously described (Appendix A):

$$y_t(t) = A_1\cos\left(w_s t + \theta_2\right) + A_2\cos(2w_s t) + A_3 + A_4 t + A_5 t^2 + A_6 t^3$$

Where w_s is the frequency of the first harmonic (H1), θ_2 is the phase shift of H1 relative to H2, A_1 and A_2 are the amplitudes of H1 and H2

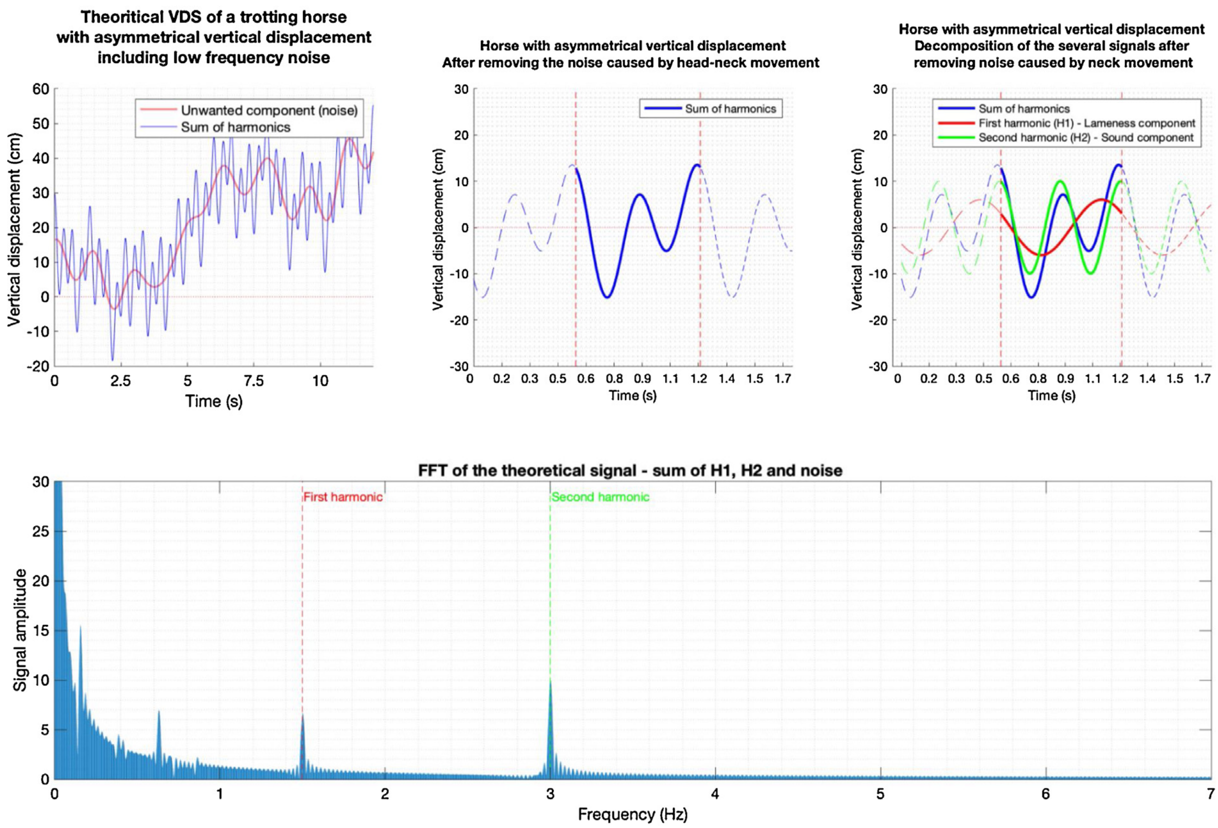

Fig. 1. The resulting measured signal is the sum of the two harmonics and the unwanted components resulting from the random non-periodic neck/head movement of the horse during trot locomotion. Top left: the measured signal (red) and the noise signal (blue). Top middle: The measured signal (blue) after removing the noise signal. Top Right: The measured signal after removing the noise, decomposed in two harmonics. Bottom: FFT of the measured signal where the signal power of the different frequencies composing the final measured signal can be observed.

respectively, A_3 is a moving average and A_{4-6} are the amplitudes of each element of a third order polynomial function.

4 The unknown coefficients are estimated using a trust-region-reflective least squares approach, using Matlab function 'lsqnonlin'. Using coefficients A_{3-6} the unwanted components present in the signal can be predicted and using the remaining coefficients, the VDS signal can be estimated.

3.4. *Designing a moving average filter*

A moving average was calculated for each frame of the data using a sliding window. Varying window lengths were tested, ranging from 0.1–6 complete strides. This filter technique was also evaluated with and without the padding technique as described in section. 1.1. The filtered signal was calculated by subtracting the moving average from the raw signal.

3.5. *Filter evaluation and optimisation*

To evaluate the performance of each filter technique, we calculated the residuals (r) between the raw and filtered signal:

$$r = p - (p \hat{+} n)$$

Where (p) represents the original clean VDS, (n) represents the unwanted components on the signal and ($p \hat{+} n$) represents the filter output of ($p + n$). This operation was performed in signals with increasing degree of asymmetry (Supplement, Fig. 2). For the IIR filters and the moving average filter we calculated residuals for incremental degrees of asymmetry (See supplement Fig. 2) and filter cut-off frequency (from 0.1 Hz to 6 Hz), thus covering the upper and lower ranges of previously described cut-off frequencies [25–28]. For the moving average filter, we have calculated residuals for incremental degrees of asymmetry and moving window length (defined as the number of strides, ranging from 0.1–6 strides). The increasing degrees of asymmetry was generated by increasing the amplitude of H1, as previously shown in horses with induced lameness [4].

3.6. *Evaluation of the different filter techniques in VDS symmetry in real data from horses, before and after lameness induction*

Based on the results of the initial investigation, we have created a procedure (Diagram 1) to evaluate the effect and performance of the different filters using real data. We have used data from a previous study [29] in which lameness had been induced in seven healthy horses (in 4 horses in a forelimb and in 3 in a hindlimb) using a modified horseshoe. This shoe consists of a heart-bar horseshoe, where an M10 screw is fitted, so the end of the screw will contact the tip of the frog (Supplement Fig. 3). Lameness is induced when the screw is inserted and tightened, applying pressure to the tip of the frog. Horses were measured in trot on a straight line, before and after lameness induction using 18 optical motion capture cameras (Oqus 700+, 200 Hz, Qualisys AB, Motion Capture Systems, Gothenburg, Sweden). Data tracking was manually validated, and the 3D coordinates of reflective markers (19 mm Ø) placed on the poll, withers and pelvis (Supplement, Fig. 4) were exported into Matlab. Stride segmentation was performed using the time index of the maximum protraction of the left hind limb [8]. Data were processed in Matlab:2017b using custom-written

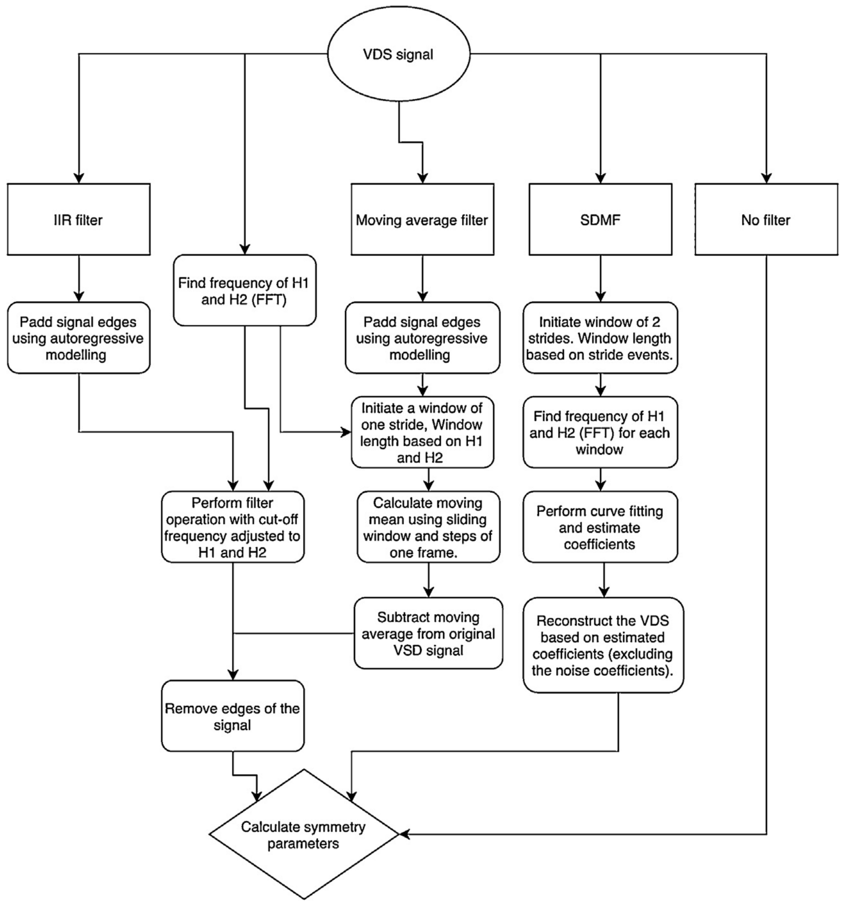

Diagram 1. Data processing and sequence of operations used to evaluate the effect and performance of each filter in the data from horses with induced lameness. VDS: Vertical displacement signal; IIR: Infinite impulse response; SDMF: Signal Decomposition method filter; FFT: Fast Fourier transformation.

scripts. Each filter was developed as described in Diagram 1 and symmetry parameters were calculated as previously described [23]. These parameters were RUD and RDD (difference in upward resp. downward movement of the head, withers and sacrum markers between the right and left halves of a stride), and MinDiff and MaxDiff (difference between right and left halves of a stride in minimum resp. maximum height of markers).

The study was approved by the local ethics committee in compliance with the Dutch Act on Animal Experimentation.

3.7. Statistics

Open software R (R-Studio, Boston, Massachusetts, USA) (version 3.3.1) was used for statistical analysis. To evaluate the effect of each filter, two linear mixed models were generated using the function lmer (lme4, version 1.1–12). The first model aimed at evaluating the effect of each filter on the mean symmetry parameter calculated for each trial. The second model aimed at evaluating the effect of each filter on between-stride variation, and its effect on the symmetry parameters calculated for each trial. Between-stride variation was defined as the median absolute deviation on a trial level. For both models, horse ID and trial within horse ID were used as random effects and the interaction between the filter and the condition (sound and lame) as a fixed effect. The outcome variables were each calculated symmetry parameter. Model estimates (least square means), confidence intervals and p-values were calculated from the models using the package lsmeans (version 2.23–5). P-values for the model outcome were corrected for multiple comparison using the false discovery rate method of Benjamini & Hochberg.

4. Results and discussion

4.1. Effects of the different filtering techniques on the theoretical VDS

All tested filters were able to remove the unwanted components of the signal to different extents (Table 1, Figs. 1 and 3). The described padding technique achieved an optimal reduction of the transient effect on the VDS edges (Table 1, Fig. 3). The degree of asymmetry did not affect the selection of the optimal cut-off frequency in our results. Choosing an appropriate value for the cut-off frequency of the IIR filters and the window size for the moving average filter, appear to be of great importance when optimising filtering techniques for the tested VDS (Fig. 1).

4.1.1. Selection of the optimal cut-off frequency

An initial investigation of the theoretical signal demonstrated that the selection of the cut-off frequency used for the IIR filter is crucial (Fig. 4). When the cut-off frequency of the filter is too low, almost no unwanted components are attenuated, as can be anticipated. On the other hand, if the cut-off frequency of the filter approaches the frequency of the first harmonic (H1), the asymmetry of the signal is reduced, and any symmetry parameters calculated after that will be affected (Fig. 4). This is also demonstrated in Fig. 2. The residual analysis shows that a clear optimal

Table 1
Descriptive statistics of the comparison of the four different filter techniques at their optimal setting RMSE: root mean square error. Mean residual as the mean of the absolute residuals (theoretical signal - filter output). *: This parameter was not tested as it is already described in the literature ([4]).

	Butterworth		Chebyshev type I		Moving average		SDMF
	with padding	without padding	with padding	without padding	with padding	without padding	
RMSE	0.24	1.29	0.05	1.35	0.99	1.17	0.17
Mean residual (mm)	−0.07	−1.21	−0.03	−1.08	−0.5	0.81	0.17
s.d. residual (mm)	2.4	77.45	0.59	13.51	9.98	11.69	1.78
Max residual (mm)	5.48	130.18	1.12	27.43	19.92	35.63	5.8
Min residual (mm)	−4.2	−147.09	−2.3	−112.21	−20.07	−20.07	−3.08
Optimal – cut-off frequency, as a % of the step frequency (H2)	36%	36%	48.7%	48.7%			
Window length (number of strides)					0.95	0.95	2 *

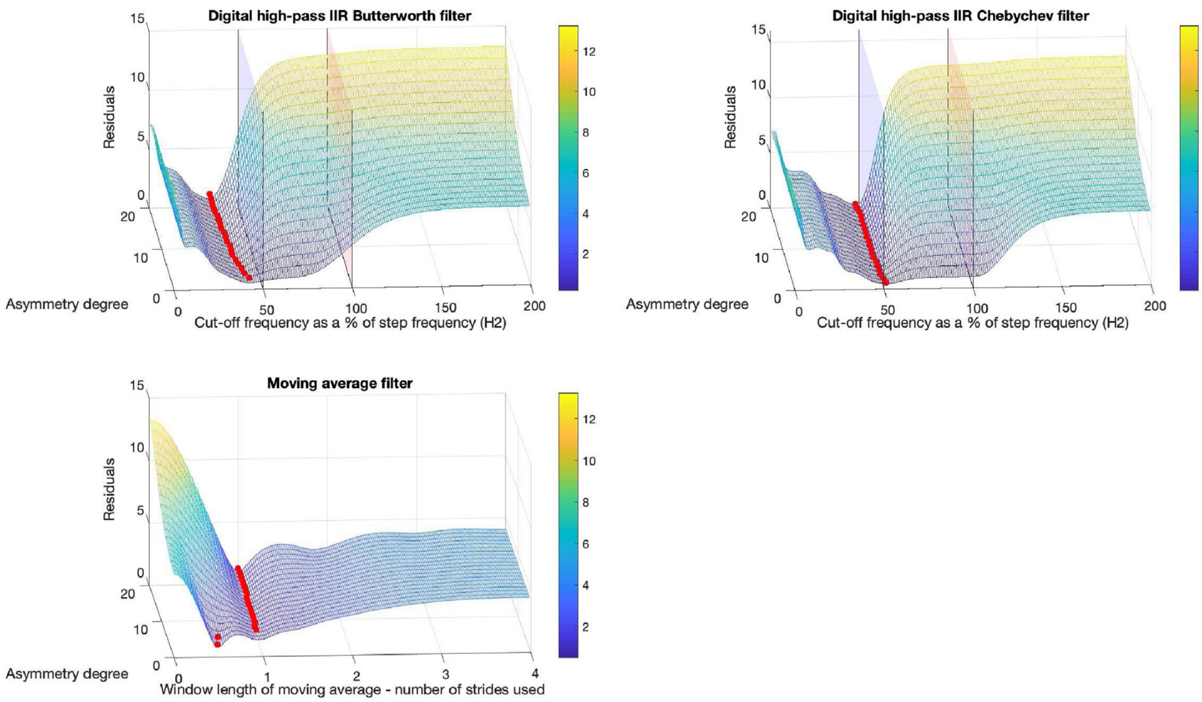

Fig. 2. 3D mesh plot of the filter residuals (z-axis) against increasing filter order (y-axis) and increasing cut-off frequency (x-axis) for both Butterworth and Chebyshev type I filters. The points with the lowest residuals are indicated in red.

cut-off frequency can be achieved (Table 1), and this frequency is below the frequency of H1 (stride frequency).

Suboptimal selection of the cut-off frequency, aproaching or even above the frequency of H1 can, in theory, result in false negative results when this technique is used to evaluate motion symmetry due to lameness. This has not always been acknowledged explicitly in earlier research where a set cut-off frequency was used for IIR filters [25–28]. However, in these publications, the chosen cut-off frequencies were below the expected stride frequency (H1) for trotting horses, so no considerable reduction of asymmetry can be expected to have occurred. Nevertheless, it is crucial to determine the optimal cut-off frequency for each signal, since the frequency of each harmonic is dependent on the speed of the horse [30] as well as individual horses can have rather different stride frequencies, within the same speed. Higher speeds are related to higher stride frequencies (H1), and if the preset cut-off frequency is too low in relation to the frequency of H1, this might result in a suboptimal noise reduction and higher values of between-stride variation.

Another crucial factor is that, when the cut-off frequency is selected for a specific signal, it is assumed that the frequency of the signal does not change over time. For measurements performed on a treadmill this is generally the case, as belt speed can be adjusted and maintained. However, measurements overground are subject to variations in speed over time (Fig. 5), which will affect the frequency of the signal components H1 and H2. When a high variation in speed is present within a measurement, IIR filters might not be the optimal solution since they work on a frequency domain.

It should be noted that the approach for filter optimisation described above was applied to theoretical signals. In this context, it is important to state that the optimal cut-off frequency is most likely dependent on the different unwanted components present in the VDS and thus can be different under other conditions. Therefore, the results here described should be used as guidelines and not seen as a strict rule. We advise readers to study their signals and adjust their filter settings accordingly. Nevertheless, the use of standardised methods for signal analysis allows for the better comparison of measurements from different studies and will increase reproducibility.

4.1.2. *Effect of filter transients when using IIR filters*

The effect of filter transients when using IIR filters is well described. As seen in Fig. 3, the edges of the filtered signal can be severely affected, which may ultimately result in erroneous symmetry calculations. To overcome this problem, our proposed method of autoregressive modelling of the edges of the signal suc-

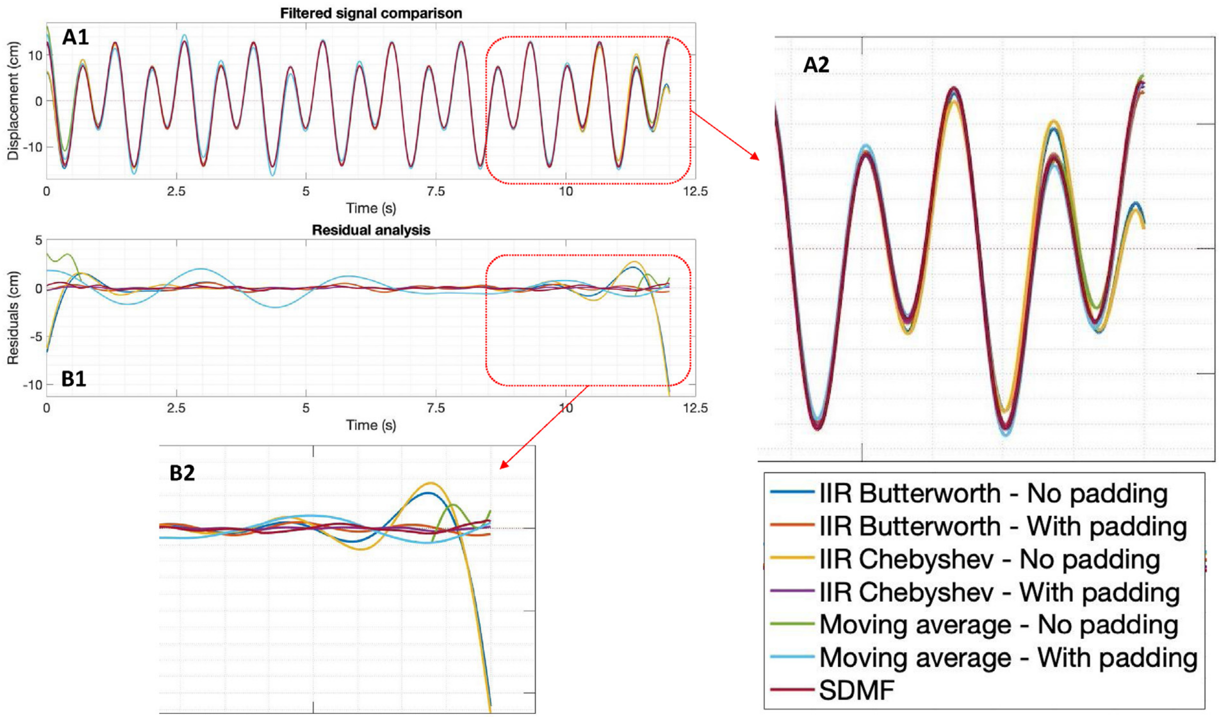

Fig. 3. Comparison of the output from the different methods of filtering **A1** and residual analysis **B1**. **A2**: detailed comparison of the output from the different methods of filtering on the signal edges (note the effect of filter transients when no padding is used). This can also be appreciated in the signal edges from the residual analysis (**B2**).

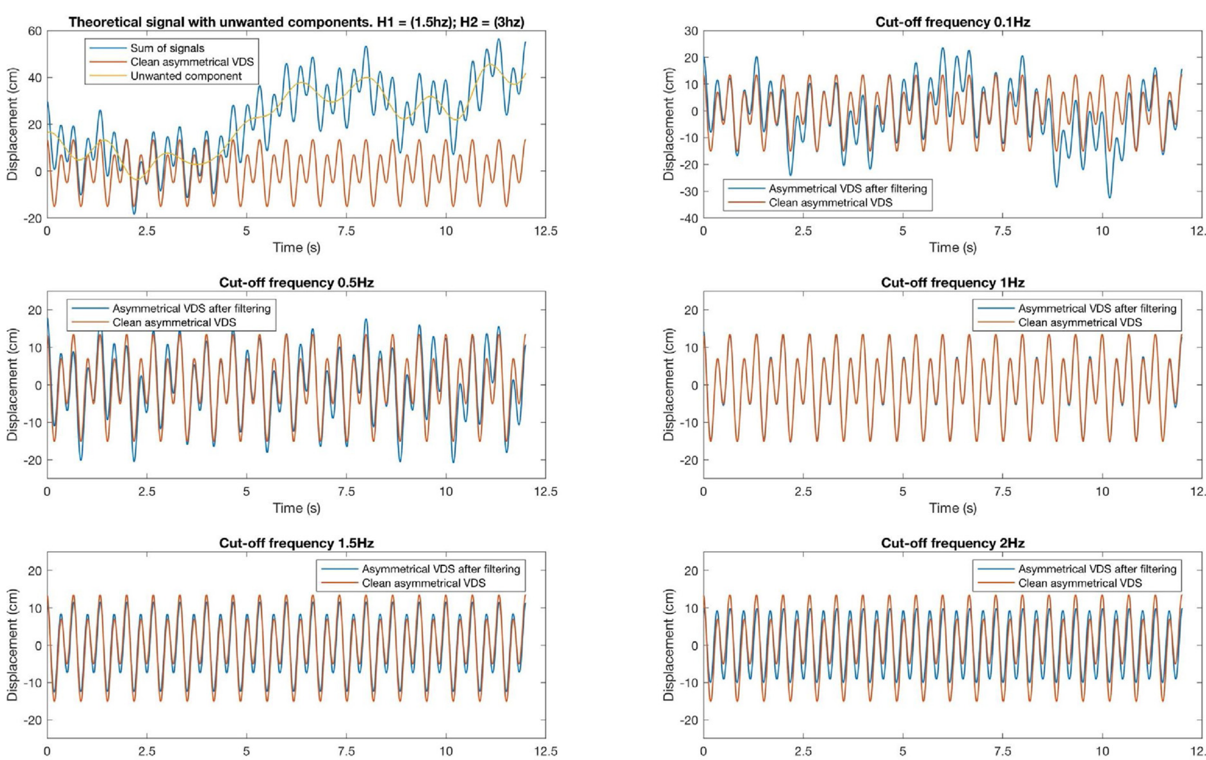

Fig. 4. The effect of cut-off frequency on a theoretical vertical displacement signal (VDS), with an H1 frequency of 1.5 Hz and H2 of 3 Hz. The filter used was a 4th order IIR high-pass Butterworth, using a zero-phase function, with a cut-off frequency set to 0.1 Hz (top right), 0.5 Hz (middle left), 1 Hz (middle right), 1.5 Hz (bottom left) and 2 Hz (bottom right). Note the reduction of the asymmetry of the signal once the cut-off frequency approaches the frequency of the first harmonic (H1). At 2 Hz, the asymmetry is no longer present.

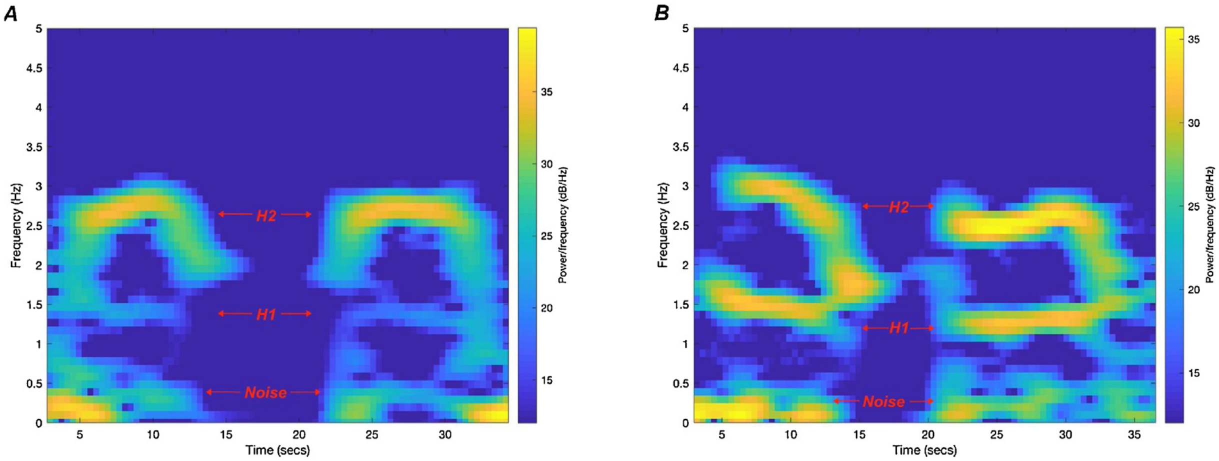

Fig. 5. Spectrogram of the vertical displacement signal from a horse trotting overground, before (A) and after (B) lameness induction. Each plot consists of two runs, with a period where the horse stopped between the runs. Note that the frequencies of H1 and H2 are not constant throughout the measurement due to variations in speed. Also, note the increased amplitude (Power) of H1 after lameness induction.

cessfully resulted in removing the effect of filter transients, while preserving all available strides from a measurement and not affecting the optimal cut-off frequency (Table 1).

An additional approach to mitigate this can be excluding the first and last stride(s) of a measurement. Removing the first and last stride(s) might also be useful in measurements where there are large variations in speed, which ultimately might cause an increase in between-stride variation. However, if the number of available strides for a specific measurement is small, which is often the case for gait analysis using optical motion capture (due to the number of cameras available to record several consecutive strides), this solution is less than optimal. Gait analysis systems using sensors attached to the horse (e.g. accelerometers) generally do not suffer from this limitation to the same extent, since quite often, more strides are easily recorded with such systems using wireless data transmission or continuous on-board data logging.

4.1.3. Filter effects in real data from horses with induced lameness: effect on the commonly calculated symmetry parameters

Our results suggest that the choice of filtering technique has mainly an effect on the between-stride variation. In our results, this is confirmed by an overall reduction in between-stride variation on the calculated symmetry parameters for all filters, when compared to the no filter situation. Fig. 6 illustrates the effect of each filter technique on the MinDiff of the head, withers and pelvis VDS before (sound) and after (lame) lameness induction. Tables 2 and 3 describe the detailed model estimates and the comparison of the performance of the different outputs (Diagram 1).

Regarding the between-stride variation, all tested filter techniques were able to significantly reduce this source of variation in the symmetry parameters, when compared to no filter (Table 2). The filter effect was more pronounced on the symmetry parameters of the head, and withers, when compared to the sacrum. A higher natural between-stride variation has previously been reported for the head [9]. This was also obvious in our data, where the model estimates for all filters were smaller for the pelvis symmetry between-stride variation when compared to the head. The Butterworth and the SDMF filters performed well for all body parts, with the SDMF achieving in some occasions, greater reduction of between-stride variation (Table 2), although the difference between the Butterworth and SDMF was not statistically significant (comparison not shown). We hypothesise, as the authors who originally published the technique [4], that the small difference in favour of the SDMF is due to the continuous adjustment to the stride frequency for each curve fitting operation (Diagram 1). Therefore, the technique is well-suited when a measurement takes place overground, during which changes in trotting speed may occur naturally (Fig. 5). Since the IIR filters need to be tuned to the frequency of the entire VDS of the measurement, these might fail to remove some of the unwanted components of the signal. While technically performing slightly better, the SMDF has a main drawback that affects user friendliness. The IIR filters outperform the SMDF regarding the speed with which the filter operation is performed because the SDMF filter requires several optimisations and curve-fitting operators that are comparatively computer intensive.

We also found overall smaller values for between-stride variation, independent of the filter technique used, for horses after lameness induction, compared to before (Table 2). In other words, when horses are suffering from orthopaedic pain, the between-stride variation is reduced as an effect of pain. This explains why the filter effect is more obvious before lameness induction. The phenomenon of low stride variability in animals with orthopaedic pain has been observed previously [31], and can possibly be related to constrained movements, as an attempt to reduce variation in speed and acceleration.

Regarding the mean asymmetry values calculated, the filter technique has more pronounced effects on the head and withers for some of the parameters (Table 3). Interestingly, this was more obvious for the head and withers before lameness induction. This finding is in line with the reasoning above and highlights that the filtering operation does not affect the true asymmetry present in the signal and that its primary function is to reduce the unwanted components present in the signal and to calculate asymmetry parameters with higher overall precision.

One important factor that was not evaluated in this study is the relation between between-stride variation of symmetry parameters and the number of collected strides. It can be anticipated that in measurements where a high between-stride variation is present, a higher confidence in the calculated symmetry values can be achieved by collecting more strides. There are likely a number of confounding factors related to this such as variations in acceleration/speed and demeanor as well as a gradual change in movement asymmetry when a horse is ‘warming out of’ a lameness or the lameness increases with repeated loading cycles. This evaluation was beyond the scope of this manuscript, but further research is needed to fully understand the relation between between-stride variation and the number of collected strides.

Table 2

Model estimates and p-value for filter effects on between-stride variation. p-values for the comparison with the 'No Filter' condition. RUD and RDD (difference in upward resp. downward movement of the head, withers and sacrum markers between the right and left halves of a stride). MinDiff and MaxDiff (difference between right and left halves of a stride in minimum resp. maximum height of markers).

				MinDiff				MaxDiff				Range Up Difference (RUD)				Range Down Difference (RDD)			
				Lsmean	Lower C.I	Upper C.I	p-value	Lsmean	Lower C.I	Upper C.I	p-value	Lsmean	Lower C.I	Upper C.I	p-value	Lsmean	Lower C.I	Upper C.I	p-value
Between stride variation (MAD)	Head	Sound	No Filter	30.5	23.2	37.7	–	33.5	27.6	39.5	–	29.3	19.9	38.7	–	28.3	21.0	35.6	–
			Butterworth	17.6	10.3	24.9	<0.001	14.0	8.1	19.9	<0.001	21.9	12.5	31.3	0.02	21.5	14.2	28.8	<0.001
			Chebychev	20.6	13.3	27.8	0.004	16.9	11.0	22.8	<0.001	24.1	14.7	33.6	0.1	24.4	17.1	31.7	0.1
			SDMF	17.6	10.3	24.8	<0.001	14.3	8.3	20.2	<0.001	21.9	12.5	31.4	0.02	20.8	13.5	28.1	<0.001
			Moving Average	17.9	10.6	25.1	<0.001	15.9	9.9	21.8	<0.001	26.0	16.6	35.5	0.3	23.6	16.3	30.9	0.02
		Lame	No Filter	33.0	25.8	40.3	–	30.1	24.2	36.1	–	30.5	21.0	39.9	–	27.4	20.1	34.7	–
			Butterworth	17.2	10.0	24.5	0.5	11.8	5.9	17.8	0.8	19.7	10.2	29.1	0.4	19.0	11.7	26.3	0.6
			Chebychev	22.4	15.1	29.7	0.9	15.9	9.9	21.8	0.7	27.0	17.6	36.4	0.7	23.3	16.0	30.6	0.9
			SDMF	17.9	10.6	25.1	0.6	11.6	5.7	17.6	0.9	20.5	11.1	29.9	0.6	19.6	12.3	26.9	0.9
			Moving Average	19.7	12.5	27.0	0.9	15.3	9.4	21.3	0.6	23.1	13.6	32.5	0.3	23.1	15.8	30.4	0.9
	Withers	Sound	No Filter	11.2	9.7	12.7	–	13.7	12.3	15.2	–	19.5	17.3	21.8	–	20.4	18.6	22.1	–
			Butterworth	5.2	3.7	6.6	<0.001	6.3	4.8	7.7	<0.001	7.7	5.5	9.9	<0.001	7.5	5.8	9.3	<0.001
			Chebychev	5.5	4.1	7.0	<0.001	7.5	6.0	8.9	<0.001	9.5	7.3	11.7	<0.001	9.6	7.8	11.4	<0.001
			SDMF	5.0	3.6	6.5	<0.001	6.2	4.8	7.7	<0.001	7.9	5.7	10.1	<0.001	7.8	6.0	9.6	<0.001
			Moving Average	5.7	4.2	7.2	<0.001	7.8	6.3	9.2	<0.001	8.4	6.2	10.6	<0.001	9.0	7.2	10.8	<0.001
		Lame	No Filter	10.8	9.4	12.3	–	10.3	8.8	11.7	–	20.2	18.0	22.4	–	20.4	18.6	22.2	–
			Butterworth	4.5	3.0	5.9	0.8	4.5	3.1	6.0	0.1	6.6	4.4	8.8	0.4	6.4	4.6	8.2	0.5
			Chebychev	5.1	3.7	6.6	1.0	5.9	4.5	7.3	0.04	8.2	6.0	10.4	0.3	7.9	6.1	9.6	0.2
			SDMF	4.6	3.2	6.1	1.0	4.7	3.2	6.1	0.04	7.0	4.8	9.3	0.4	6.4	4.6	8.2	0.4
			Moving Average	4.9	3.4	6.4	0.7	5.4	4.0	6.8	0.2	6.8	4.6	9.0	0.2	7.0	5.2	8.8	0.2
	Pelvis	Sound	No Filter	11.6	9.7	13.6	–	14.0	11.1	16.8	–	13.5	11.3	15.7	–	15.2	11.4	19.1	–
			Butterworth	7.9	6.0	9.9	<0.001	8.5	5.6	11.3	<0.001	11.8	9.6	14.0	0.1	13.5	9.6	17.3	0.3
			Chebychev	7.9	5.9	9.8	<0.001	8.2	5.3	11.0	<0.001	11.8	9.6	14.0	0.1	14.2	10.3	18.0	0.5
			SDMF	7.7	5.8	9.7	<0.001	6.3	3.4	9.1	<0.001	8.5	6.3	10.7	<0.001	11.1	7.2	14.9	0.01
			Moving Average	9.5	7.6	11.5	0.04	8.8	6.0	11.7	<0.001	12.8	10.6	15.0	0.5	15.3	11.5	19.2	1.0
		Lame	No Filter	11.0	9.0	12.9	–	10.2	7.4	13.1	–	9.6	7.4	11.8	–	10.0	6.1	13.8	–
			Butterworth	5.4	3.5	7.4	0.2	5.6	2.7	8.4	0.7	10.1	7.9	12.3	0.2	8.4	4.5	12.2	0.9
			Chebychev	6.7	4.7	8.6	0.7	7.2	4.4	10.1	0.2	9.8	7.6	12.0	0.2	9.3	5.4	13.1	0.9
			SDMF	5.3	3.4	7.3	0.2	6.2	3.4	9.1	0.1	7.0	4.8	9.2	0.1	8.5	4.7	12.4	0.2
			Moving Average	6.1	4.1	8.0	0.1	6.8	4.0	9.7	0.4	9.5	7.3	11.7	0.7	9.8	5.9	13.6	0.9

Table 3
Model estimates and p-value for filter effect on absolute mean asymmetry. p-values for the comparison with the 'No Filter' condition. RUD and RDD (difference in upward resp. downward movement of the head, withers and sacrum markers between the right and left halves of a stride). MinDiff and MaxDiff (difference between right and left halves of a stride in minimum resp. maximum height of markers).

				|MinDiff|				|MaxDiff|				|Range Up Difference (RUD)|				|Range Down Difference (RDD)|			
				Lsmean	Lower C.I	Upper C.I	p-value	Lsmean	Lower C.I	Upper C.I	p-value	Lsmean	Lower C.I	Upper C.I	p-value	Lsmean	Lower C.I	Upper C.I	p-value
Mean symmetry value	Head	Sound	No Filter	10.8	−2.8	24.4	–	12.4	2.5	22.2	–	18.2	−0.5	36.9	–	6.9	−2.3	16.0	–
			Butterworth	8.8	−4.8	22.4	0.09	9.0	−0.8	18.8	0.005	16.5	−2.3	35.2	0.04	5.7	−3.4	14.9	0.1
			Chebychev	9.3	−4.3	22.9	0.21	9.6	−0.2	19.4	0.02	17.5	−1.2	36.2	0.4	6.2	−2.9	15.4	0.4
			SDMF	8.4	−5.2	22.0	0.05	7.9	−1.9	17.7	<0.001	15.9	−2.8	34.6	0.01	5.7	−3.5	14.8	0.1
			Moving Average	8.8	−4.8	22.4	0.10	9.4	−0.4	19.2	0.01	16.9	−1.8	35.7	0.1	6.2	−2.9	15.4	0.3
		Lame	No Filter	39.7	26.1	53.3	–	23.1	13.3	32.9	–	60.0	41.3	78.7	–	26.8	17.7	35.9	–
			Butterworth	36.2	22.6	49.8	0.35	22.0	12.2	31.8	0.2	56.1	37.4	74.8	0.1	24.4	15.3	33.6	0.2
			Chebychev	36.9	23.3	50.5	0.41	23.4	13.6	33.2	0.1	58.9	40.2	77.6	0.8	25.0	15.9	34.2	0.2
			SDMF	36.6	23.0	50.2	0.64	22.1	12.3	31.9	0.03	56.6	37.9	75.3	0.4	24.7	15.6	33.8	0.3
			Moving Average	37.2	23.6	50.8	0.71	22.4	12.6	32.2	0.2	58.2	39.5	76.9	0.7	25.5	16.4	34.6	0.5
	Withers	Sound	No Filter	4.5	1.0	8.0	–	11.2	5.6	16.8	–	7.0	0.7	13.4	–	14.3	5.6	23.1	–
			Butterworth	4.6	1.0	8.1	0.90	9.7	4.0	15.3	<0.001	7.4	1.0	13.7	0.6	12.8	4.0	21.6	0.04
			Chebychev	4.7	1.2	8.3	0.61	9.9	4.3	15.6	<0.001	7.6	1.3	14.0	0.4	13.2	4.4	22.0	0.1
			SDMF	4.6	1.1	8.2	0.79	9.5	3.9	15.1	<0.001	7.4	1.1	13.8	0.6	12.7	4.0	21.5	0.03
			Moving Average	4.6	1.1	8.2	0.76	10.0	4.4	15.7	<0.001	8.0	1.7	14.4	0.1	13.1	4.3	21.9	0.1
		Lame	No Filter	15.3	11.8	18.9	–	9.1	3.5	14.8	–	12.3	6.0	18.7	–	20.2	11.5	29.0	–
			Butterworth	14.8	11.3	18.3	0.33	7.9	2.3	13.5	0.6	12.1	5.8	18.5	0.6	19.7	10.9	28.5	0.3
			Chebychev	15.7	12.1	19.2	0.85	8.5	2.8	14.1	0.2	12.7	6.4	19.1	0.8	21.0	12.2	29.8	0.1
			SDMF	14.8	11.2	18.3	0.25	7.7	2.1	13.3	0.6	12.1	5.7	18.4	0.5	20.0	11.2	28.8	0.2
			Moving Average	15.2	11.6	18.7	0.61	8.3	2.7	13.9	0.5	12.4	6.0	18.7	0.3	20.2	11.4	28.9	0.3
	Pelvis	Sound	No Filter	4.5	−3.5	12.5	–	5.6	−3.0	14.1	–	6.7	−7.5	21.0	–	6.6	1.6	11.7	–
			Butterworth	5.0	−3.0	13.1	0.40	4.6	−3.9	13.1	0.1	6.0	−8.2	20.3	0.4	6.2	1.1	11.2	0.6
			Chebychev	5.3	−2.7	13.3	0.23	4.5	−4.0	13.0	0.04	6.3	−7.9	20.6	0.6	6.1	1.1	11.2	0.6
			SDMF	5.0	−3.0	13.1	0.42	4.0	−4.5	12.6	0.004	7.8	−6.5	22.1	0.2	7.6	2.6	12.7	0.3
			Moving Average	5.2	−2.9	13.2	0.31	4.9	−3.6	13.5	0.2	6.5	−7.8	20.8	0.8	6.7	1.7	11.8	0.9
		Lame	No Filter	17.0	9.0	25.0	–	16.2	7.7	24.8	–	32.8	18.5	47.0	–	10.4	5.4	15.5	–
			Butterworth	15.6	7.6	23.7	0.04	14.1	5.5	22.6	0.1	30.0	15.7	44.3	0.1	9.8	4.7	14.8	0.9
			Chebychev	16.6	8.6	24.6	0.20	15.0	6.5	23.5	0.8	31.8	17.5	46.1	0.6	10.0	5.0	15.1	0.9
			SDMF	15.4	7.4	23.4	0.03	14.8	6.3	23.3	0.9	31.4	17.1	45.6	0.03	10.5	5.5	15.6	0.5
			Moving Average	16.0	8.0	24.1	0.08	14.7	6.1	23.2	0.2	31.1	16.8	45.3	0.2	10.0	5.0	15.1	0.7

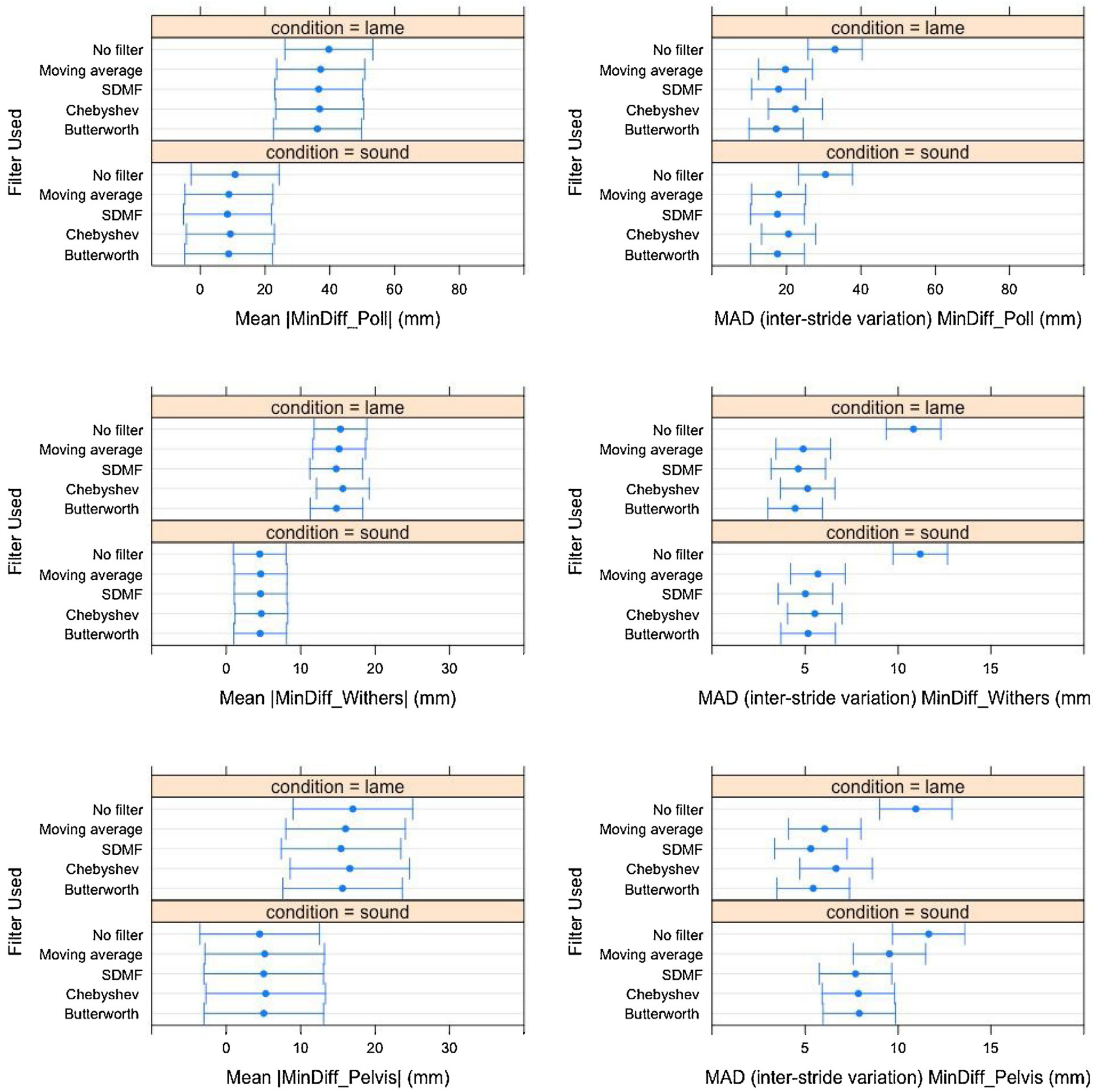

Fig. 6. Least square means (blue dot) and confidence intervals (error bar) for the two models, for the symmetry parameter MinDiff, for head, withers and pelvis.

5. Conclusions

This study shows the importance of choosing appropriate signal analysis techniques, when processing data acquired using quantitative gait analysis equipment and how these choices may influence commonly used symmetry parameters for objective lameness assessment in horses. Cut-off frequencies that are very close or even higher than the frequency of the first harmonic (H1) of the VDS will, depending on the filter type that is used, ultimately distort the measured signal and may result in mean calculated symmetry outside the reference values. On the other hand, when filter operations are suboptimal, this can result in higher between-stride variation that can affect the significance of calculated symmetry parameters. There is hence a considerable impact of filtering on the calculated parameters used for objective lameness assessment, and detailed knowledge of how filters work and what effects their applications may have is a prerequisite for any biomechanical researcher working in this field. Further work is needed to better understand the biological significance of all the different components of the VDS of trotting horses and further signal analysis techniques such as wavelet analysis should be then implemented.

Sources of funding

Swedish Research Council Formas funded the study (2014-12003-28225-26).

Acknowledgement

We would like to thank Prof. Kevin Keegan for his valuable input during the development of this manuscript.

Declaration of Competing Interest

C. Roepstorff is an employee of Qualisys AB. No other author of this manuscript has a financial or personal relationship with other people or organisations that could inappropriately influence or bias the content of the paper.

Appendix A.

The VDS of a horse during trot can be thought of as a harmonic oscillator described by the equation:

$$F(t) = -ky(t)$$

where k is the spring constant and y is the displacement. Together with Newton's second law,

$$F(t) = m\frac{d^2y(t)}{dt^2}$$

we get a differential equation on the form,

$$m\frac{d^2y(t)}{dt^2} + ky(t) = 0$$

which has the solution

$$y(t) = A.cos(wt + \theta)$$

where A_2 A is the amplitude of the sinusoid, $w = \sqrt{\frac{k}{m}}$ $\mathrm{w} = \sqrt{\frac{\mathrm{k}}{\mathrm{m}}}$ and θ θ is the phase shift. We define w_s $\mathrm{w_s}$ as the angular frequency of the horse's stride, thus leading to an equation describing the symmetric step component of the movement (H2),

$$y_1(t) = A_2\cos(2w_st + \theta_1)$$

When a horse is experiencing orthopaedic pain, this motion cycle becomes asymmetrical [3,22]. This asymmetric stride component (H1) of the movement can be theoretically described as:

$$y_2(t) = A_1\cos(w_st + \theta_2)$$

The total vertical displacement, including both the step ($2w_s$) and stride w_s frequency component, ends up as the sum of the last two equations:

$$y_t(t) = A_1\cos\left(w_st + \theta_2\right) + A_2\cos\left(2w_st + \theta_1\right)$$

As the phase shift describes how the two sinusoids are shifted about what is considered zero in time, we can, for the sake of simplicity, define t_0 $\mathrm{t_0}$ to always occur so that $\theta_1 = 0$ $\theta_1 = 0$, resulting in the following formula:

$$y_t(t) = A_1\cos\left(w_st + \theta_2\right) + A_2\cos(2w_st)$$

where A_1 $\mathrm{A_1}$ is the amplitude of the asymmetric (H1) component, A_2 $\mathrm{A_2}$ is the amplitude of the symmetric (H2) component and θ_2 θ_2 is the phase shift of the asymmetric stride component.

When a horse is trotting overground and to a smaller extend also on a treadmill, additional unwanted components $n_t(t)$ $\mathrm{n_t(t)}$ are added to this signal. These are mainly due to the random noncyclical motion unrelated to the primary locomotion movement or due to non-horizontal ground reference (e.g. if the horse is moving on an inclined plane). Previously [4,24], these unwanted components have been described as a sum of a moving average (C_1), and a third order polynomial function:

$$n_t(t) = C_1 + \sum_{K=1}^{3} A_k t^k$$

Therefore, the final description of the VDS of a moving horse will be the sum of the two equations describing both the dorsoventral movement (sum of the first [H1] and second [H2] harmonic) of the horse and the unwanted components of the movement as follows:

$$y_t(t) = A_1\cos\left(w_st + \theta_2\right) + A_2\cos(2w_st) + A_3 + A_4t + A_5t^2 + A_6t^3$$

Appendix B. Supplementary data

Supplementary material related to this article can be found, in the online version, at doi:https://doi.org/10.1016/j.bspc.2019.101674.

References

[1] F.M.M. Serra Bragança, M. Rhodin, P.R.R. van Weeren, On the brink of daily clinical application of objective gait analysis: What evidence do we have so far from studies using an induced lameness model? Vet. J. 234 (2018) 11–23, http://dx.doi.org/10.1016/j.tvjl.2018.01.006.

[2] P.R. van Weeren, T. Pfau, M. Rhodin, L. Roepstorff, F. Serra Bragança, M.A. Weishaupt, Do we have to redefine lameness in the era of quantitative gait analysis? Equine Vet. J. 49 (2017) 567–569, http://dx.doi.org/10.1111/evj.12715.

[3] H.H.F. Buchner, H.H. Savelberg, H.C. Schamhardt, A. Barneveld, Head and trunk movement adaptations in horses with experimentally induced fore- or hindlimb lameness, Equine Vet. J. 28 (1996) 71–76, http://dx.doi.org/10.1111/j.2042-3306.1995.tb04911.x.

[4] K.G. Keegan, P.F. Pai, Da Wilson, B.K. Smith, Signal decomposition method of evaluating head movement to measure induced forelimb lameness in horses trotting on a treadmill, Equine Vet. J. 33 (2001) 446–451, http://dx.doi.org/10.2746/042516401776254781.

[5] C. Peham, T. Licka, D. Girtler, M. Scheidl, Supporting forelimb lameness: clinical judgement vs. computerised symmetry measurement, Equine Vet. J. 31 (1999) 417–421.

[6] J.G. Peloso, J.A. Stick, R.W. Soutas-Little, J.C. Caron, C.E. DeCamp, D.H. Leach, Computer-assisted three-dimensional gait analysis of amphotericin-induced carpal lameness in horses, Am. J. Vet. Res. 54 (1993) 1535–1543.

[7] E. Persson Sjödin, F. Serra Braganca, T. Pfau, A. Egenvall, M.A. Weishaupt, M. Rhodin, Movement symmetry of the withers can be used to discriminate primary forelimb lameness from compensatory forelimb asymmetry in horses with induced lameness, Equine Vet. J. 48 (2016) 32–33, http://dx.doi.org/10.1111/evj.64_12595.

[8] M. Rhodin, E. Persson-Sjodin, A. Egenvall, F.M. Serra Bragança, T. Pfau, L. Roepstorff, M.A. Weishaupt, M.H. Thomsen, P.R. van Weeren, E. Hernlund, Vertical movement symmetry of the withers in horses with induced forelimb and hindlimb lameness at trot, Equine Vet. J. 50 (2018) 818–824, http://dx.doi.org/10.1111/evj.12844.

[9] K.G. Keegan, J. Kramer, Y. Yonezawa, H. Maki, P.F. Pai, E.V. Dent, T.E. Kellerman, D.A. Wilson, S.K. Reed, Assessment of repeatability of a wireless, inertial sensor-based lameness evaluation system for horses, Am. J. Vet. Res. 72 (2011) 1156–1163, http://dx.doi.org/10.2460/ajvr.72.9.1156.

[10] K.G. Keegan, Y. Yonezawa, F. Pai, Da. Wilson, J. Kramer, Evaluation of a sensor-based system of motion analysis for detection and quantification of forelimb and hind limb lameness in horses, Am. J. Vet. Res. 65 (2004) 665–670, http://dx.doi.org/10.2460/ajvr.2004.65.665.

[11] J. Kramer, K.G. Keegan, G. Kelmer, D.A. Wilson, Objective determination of pelvic movement during hind limb lameness by use of a signal decomposition method and pelvic height differences, Am. J. Vet. Res. 65 (2004) 741–747, http://dx.doi.org/10.2460/ajvr.2004.65.741.

[12] T. Pfau, C. Spicer-Jenkins, R.K. Smith, D.M. Bolt, a Fiske-Jackson, T.H. Witte, Identifying optimal parameters for quantification of changes in pelvic movement symmetry as a response to diagnostic analgesia in the hindlimbs of horses, Equine Vet. J. 46 (2014) 759–763, http://dx.doi.org/10.1111/evj.12220.

[13] F. Audigié, P. Pourcelot, C. Degueurce, J.M. Denoix, D. Geiger, C. Bortolussi, Asymmetry in placement of bilateral skin markers on horses and effects of asymmetric skin marker placement on kinematic variables, Am. J. Vet. Res. 59 (1998) 938–944.

[14] B.T. Torres, D. Whitlock, L.R. Reynolds, Y.-C. Fu, J.A. Navik, A.L. Speas, A. Sornborger, S.C. Budsberg, The effect of marker location variability on noninvasive canine stifle kinematics, Vet. Surg. 40 (2011) 715–719, http://dx.doi.org/10.1111/j.1532-950X.2011.00852.x.

[15] P.R. van Weeren, a J. van den Bogert, a Barneveld, A quantitative analysis of skin displacement in the trotting horse, Equine Vet. J. Suppl. (1990) 101–109, http://dx.doi.org/10.1111/j.2042-3306.1990.tb04746.x.

[16] P.R. van Weeren, A.J. van den Bogert, A. Barneveld, Quantification of skin displacement near the carpal, tarsal and fetlock joints of the walking horse, Equine Vet. J. 20 (1988) 203–208.

[17] C. Peham, Signals from materials, in: W. Back, H.M. Clayton (Eds.), Equine Locomotion, 2013, pp. 61–71.

[18] H.C. Schamhardt, A.J. van den Bogert, W. Hartman, Measurement techniques in animal locomotion analysis, Acta Anat. (Basel). 146 (1993) 123–129.

[19] S. Schreven, P.J. Beek, J.B.J. Smeets, Optimising filtering parameters for a 3D motion analysis system, J. Electromyogr. Kinesiol. (2015), http://dx.doi.org/10.1016/j.jelekin.2015.06.004.

[20] D.A. Winter, H.G. Sidwall, D.A. Hobson, Measurement and reduction of noise in kinematics of locomotion, J. Biomech. (1974), http://dx.doi.org/10.1016/0021-9290(74)90056-6.

[21] M.F. Sepulveda Caviedes, B.S. Forbes, T. Pfau, Repeatability of gait analysis measurements in Thoroughbreds in training, Equine Vet. J. 50 (2018) 513–518, http://dx.doi.org/10.1111/evj.12802.

[22] P. Kübber, J. Kastner, D. Girtler, P.F. Knezevic, Erkenntnisse über den Einfluß der tiefen Palmarnervanästhesie auf das Gangbild des lahmheitsfreien Pferdes mit Hilfe einer kinematischen Meßmethode, Pferdeheilkunde 10 (1994) 11–21.
[23] S.D. Starke, E. Willems, Sa. May, T. Pfau, Vertical head and trunk movement adaptations of sound horses trotting in a circle on a hard surface, Vet. J. 193 (2012) 73–80, http://dx.doi.org/10.1016/j.tvjl.2011.10.019.
[24] C. Peham, M. Scheidl, T. Licka, A method of signal processing in motion analysis of the trotting horse, J. Biomech. 29 (1996) 1111–1114, http://dx.doi.org/10.1016/0021-9290(95)00179-4.
[25] T. Pfau, T.H. Witte, A.M. Wilson, A method for deriving displacement data during cyclical movement using an inertial sensor, J. Exp. Biol. 208 (2005) 2503–2514, http://dx.doi.org/10.1242/jeb.01658.
[26] S.D. Starke, S.A. May, T. Pfau, Understanding hind limb lameness signs in horses using simple rigid body mechanics, J. Biomech. 48 (2015) 3323–3331, http://dx.doi.org/10.1016/j.jbiomech.2015.06.019.
[27] S.D. Starke, K.J. Raistrick, Sa. May, T. Pfau, The effect of trotting speed on the evaluation of subtle lameness in horses, Vet. J. 197 (2013) 245–252, http://dx.doi.org/10.1016/j.tvjl.2013.03.006.
[28] S.M. Warner, T.O. Koch, T. Pfau, Inertial sensors for assessment of back movement in horses during locomotion over ground, Equine Vet. J. 42 (2010) 417–424, http://dx.doi.org/10.1111/j.2042-3306.2010.00200.x.
[29] K. Ask, J.P.A.M. van Loon, F.M. Serra Bragança, E. Hernlund, M. Rhodin, P. Haubro Andersen, Objective pain assessment during rest and locomotion in horses with two types of induced lameness, Comp. Exerc. Physiol. 14 (2018) 42.
[30] M.A. Weishaupt, H.P. Hogg, J.A. Auer, T. Wiestner, Velocity-dependent changes of time, force and spatial parameters in Warmblood horses walking and trotting on a treadmill, Equine Vet. J. 42 (2010) 530–537, http://dx.doi.org/10.1111/j.2042-3306.2010.00190.x.
[31] C. Peham, T. Licka, D. Girtler, M. Scheidl, The influence of lameness on equine stride length consistency, Vet. J. 162 (2001) 153–157, http://dx.doi.org/10.1053/tvjl.2001.0593.